

PYRITHIONE BASED FINISHES FOR CELLULOSIC TEXTILES

NEETA KUMARI



DEPARTMENT OF TEXTILE AND FIBRE ENGINEERING

INDIA INSTITUTE OF TECHNOLOGY DELHI

OCTOBER 2022

PYRITHIONE BASED FINISHES FOR CELLULOSIC TEXTILES

by

NEETA KUMARI

Department of Textile and Fibre Engineering

Submitted

in fulfillment of the requirements of the degree of

Doctor of Philosophy

to the



INDIA INSTITUTE OF TECHNOLOGY DELHI

October 2022


© Indian Institute of Technology (IITD), New Delhi, 2022

Dedicated to my Siblings

(Suman, Shobha & Mohit)

CERTIFICATE

This is to certify that the thesis entitled '**Pyrithione based finishes for cellulosic textile**' being submitted by **Ms. Neeta Kumari** to the **Indian Institute of Technology Delhi** for the award of degree **Doctor of Philosophy**, is a record of bonafide research work carried out by her. She has worked under our guidance and supervision and fulfilled the requirements for the submission of thesis which has attained the standard required for a Ph.D. degree of this institute. The results contained in this thesis have not been submitted, in part or in full, to any other university or institute for the award of any degree or diploma.



Dr. Manjeet Jassal

Professor

Department of Textile and Fibre Engineering

Indian Institute of Technology Delhi



Dr. Ashwini K. Agrawal

Professor

Department of Textile and Fibre Engineering

Indian Institute of Technology Delhi

Date: 21.10.2022

ACKNOWLEDGEMENT

There are several respectful and affectionate people who have helped me directly and indirectly in my research work during the period of my PhD at this Institute. Without their support it would have been impossible for me to accomplish my thesis. That is why I wish to dedicate this section to recognize their support.

Firstly, I would like to express my profound sense of gratitude and indebtedness to my venerated supervisors Prof. Manjeet Jassal and Prof. Ashwini K. Agrawal, Department of Textile and Fibre Engineering, Indian Institute of Technology Delhi. Their patience and support were instrumental in accomplishing this project. Their scholastic guidance, expert supervision, constant encouragement, steadfast support, affection, and inspiration made it possible to conduct the work smoothly. They have always been a constant source of encouragement and patient bearer of my mistakes. Words cannot describe the kindness and support I received from them. I feel very much honored and it has been a real privilege for me to get an opportunity to work under them.

I am indeed obliged and sincerely thank my SRC members Prof. Bhuvanesh Gupta, Dr. Rajiv K. Srivastava, Dr. Leena Neebhani for their suggestions and invaluable inputs which greatly helped me in refining my work.

I would deeply acknowledge the support I received from the University College of Medical Sciences, University of Delhi & GTB hospital, Dilshad Garden, New Delhi. I am particularly thankful to Prof. Sambit Nath Bhattacharya, Prof. Shukla Das, Dr. Taru Singh, Dr. Shyama Datt and Dr. Sujata Singh for their constant support and invaluable suggestions for my antifungal studies.

The financial assistance in the form of fellowship by the Department of Science and Technology, Government of India, under Nanomission research grant and Resil Chemicals Pvt. Ltd., Bangalore, for this research work is thankfully acknowledged. I am also sincerely thankful to Dr. Abhijit Majumdar and Mr. Mukesh Bajya from the Department of Textile and Fibre Engineering, IIT Delhi for providing the UPF measurement facility.

I wish to convey my deep regards and heartfelt thanks to the current Head of the Department (HOD), Prof. R.S. Rengasamy, the previous HODs, Prof. B. K. Behra and Prof. Ashwini K. Agrawal, and all the respected faculty members of the Department of Textile and Fibre Engineering for their cooperation in smooth completion of my academic research work. I am indebted to Dr. Bhanu Nandan, for being approachable in times of need. Besides his busy schedule his invaluable suggestions for any life problems either experimental or personal, supported me during my PhD tenure.

I feel great pleasure in thanking all the supporting (non-teaching) staff members of the department especially, Mr. Veerender, Dr. Vikas Khatkar, and Mr. B. Biswal for their technical assistance and co-operation throughout my PhD work.

I am also truly thankful to all CRF & NRF members especially to Mr. Rajesh Kumar, Ms. Aastha Sharma, Mr. Animesh Laha, and Ms. Kumud Arora for their support during my PhD experiments and studies.

I am especially thankful to Delhi Metro Rail Cooperation (DMRC), for making my travel safe and convenient.

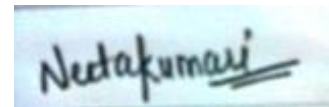
It is definitely a pleasing privilege for me to express my gratitude to my seniors Dr. Jagan Meena, Dr. Kiran Yadav, Dr. Dhirender Singh, Dr. Sidharth Sirohi, Dr. Deepika Gupta, Dr. Kamlesh Panwar, Dr. Raghav Mehra, Dr. Shipra, Dr. Rahul Mishra, and Dr. Varun Arora for their suggestions, encouragement, keen interest, and endless help at every juncture of need.

I wish to express a special word of thanks to my dear friends Dr. Puhup Puneet, Dr. Gaurav Khandelwal, Dr. Firdaus Parveen, Dr. Shashank Bahri, Dr. Bhavana Sharma, Mr. Rajesh Kumar, Ms. Nayana Janardana, and Dr. Jincy Joy for sharing all the laughter and tears together and for making my life here a memorable one as we had a wonderful time together. I would also like thank my loving fellow mates Mr. Hardeep Singh Jinjher, Dr. Rashi Agarwal, Dr. Avinash Raulo, Dr. Sanchayan Pal, Dr. Anil Yadav, Mr. Pramod, Dr. Sajjan Singh, and Dr. Shivender Singh who sailed along with me during my PhD tenure. We all may seem to have different journeys but we shared all kinds of ups and down together. I wish to express thanks to all my loving lab mates, Mr. Hardeep Singh Jinjher, Ms. Gurneet Kaur, Mr. Karan Chandrakar, Ms. Kiran Rana, Mr. Pranay Ahuja, Mr. Akhilesh Sharma, Mr. Gopal, Mr. Ram Devendra Agrawal, Mr. Shubham, and Mr. Jogender for maintaining the decorum of the lab which allowed me to carry out my work smoothly. Each one of you have a special place in my life and really made my stay at IIT a memorable and enjoyable one. I am also thankful to supporting staff of SMITA research lab Mr. Praveen and Mr. Arvind.

I cannot forget the unspoken support and encouragement from ex-smitians, Mr. Shiven Kaushal, Ms. Surabhi Jha, Mr. Garvit Sehdev, Mr. Mukul Varshney, Ms. Aparagita, Mr. Getachew, Mr. Alok, Mr. Amit Patel, Ms. Ankita Parmanick, Mr. Ramesh, and Ms. Kirti Sisodia, Mr. Manish Shukla, and Mr. Meharchand to whom I am truly thankful. The memories we spent together are deeply rooted in my life.

Words cannot express my gratitude for my parents, Mr. Jiwdhan Prajapati and Mrs. Kamla Devi for making me capable of reaching this height of education. I owe to the moral support and encouragement they have showered on me and making me what I am today. A stock of loving appreciation is reserved for my siblings, Suman Chakraverti, Shobha Prajapati, Mohit Prajapati and my dear ones, Mr. Sanjay Kumar (elder brother, friend, and supporter) and Disha Marwah for their constant support and help. A big thanks to my beloved husband, Mr. Manoj Prajapati for his constant support and encouragement during this tenure.

With deepest gratitude and love, I bow down to the Lord for never leaving me alone during the times of trials and suffering and molding me in what I am today. Last but not the least, I am thankful to all those whom I may have missed mentioning their names but may have directly or indirectly contributed to the accomplishment of this research work.

A rectangular box containing a handwritten signature in black ink. The signature reads "Neeta Kumari" with a double underline under the name "Neeta".

Neeta

ABSTRACT

Advancements in textiles by creating new functionality is in demand. Textiles are the most attractive candidate for safeguarding skin of a wearer from environmental damage, such as harmful UV rays, pollution (particulate matters), chemicals (ammonia, hydrogen sulphide etc.), microorganisms and other commonly faced topical issues. Globally, the population is suffering from severe health hazards created due to various pathogens. Apart from biological attacks, the climatic change, such as ozone layer depletion, allows harmful rays of Sun (UV-A & UV-B) to reach the Earth's surface causing skin diseases. Therefore, the emergence of effective multifunctional protective textiles has become crucial for the safety of people.

The essential aspect is that the functionality needs to be durable to washing and should not affect the comfort properties and aesthetics of the substrates. In this study, the phosphate derivative of cellulose has been explored as a linking moiety to attached functional groups.

Initially, a green chemistry approach for phosphorylation of cellulose, under atmospheric pressure plasma was investigated and compared with conventional thermal method. The attachment of the phosphate groups was evaluated by ^{31}P and ^{13}C solid state NMR spectroscopy and XPS. The thermal method led to the formation of monophosphate of cellulose along with a side product of polymerized phosphate, whereas the plasma method produced only the monophosphate without any side products. Unlike with the thermal treatment, the appearance and the mechanical properties of the viscose fabric remained nearly same after the plasma treatment. Also, the dyeability of the plasma modified fabric remained unchanged, whereas it decreased significantly in the thermally modified fabric. The amount of

phosphate quantified by phosphomolybdate assay was found to be 2.88 ± 0.06 and 4.09 ± 0.19 % in the plasma and the thermal methods, respectively. This method has the potential to replace the existing methods of phosphorylation of cellulose.

Further, considering the public health demands for stronger and effective personal protective clothing, antimicrobial fabrics using a known bacteriostatic and fungistatic drug zinc pyrithione (ZPT) has been investigated. ZPT was synthesized *in-situ* on cellulosic fabric, viscose (VC), using zinc metal precursor and 2-mercaptopyridine-N-oxide as a ligand (VC-ZPT). For comparison, viscose was also phosphorylated (VP) before *in-situ* functionalization with ZPT (VP-ZPT). Both approaches provided adequate protection from microbes, however, functionalization of cellulose with phosphate (VP) resulted in the formation of a linking group between cellulose and ZPT, which exhibited better uniformity of ZPT over the fabric surface and higher durability to washing. The functionalization was confirmed by ICP-MS, SEM and Raman spectroscopy. Further the bonding of phosphate with ZPT was confirmed by ^{31}P solid-state NMR. The physical properties, such as appearance, bending length and mechanical strength, of the treated fabrics remained unchanged. The antimicrobial activities of VP-ZPT with VC-ZPT were studied against *E. coli*, *S. aureus* and *C. albicans*, which were found to be effective till 20 laundry cycles in VP-ZPT. Additionally, VP-ZPT samples exhibited poor adherence of bacteria on the fabric surface.

Repurposing of antimicrobial metal pyrithione complexes for UV protective properties widens the applicability of protective textiles. Therefore, UV-protective and antimicrobial properties of cellulosic (viscose) textiles modified with various metal pyrithione complexes have also been investigated. Different metal (silver (Ag), cerium (Ce), copper (Cu), magnesium (Mg) and zinc (Zn)) pyrithione complexes have been *in-situ* synthesized on viscose (VC-MPT) as

well as on phosphorylated viscose (VP-MPT). The surface morphology was characterized by FE-SEM and chemical nature was studied by XRD, Raman spectroscopy, ICP-MS and solid-state NMR. The antimicrobial activities of different VC-MPT and VP-MPT treated fabrics were compared against *E. coli*, *S. aureus* and *Candida albicans* and found to be effective to various degrees (up to 98-99% microbial growth inhibition) based on the metal used. Additionally, the functionalized fabrics were found to have high UV blocking properties. The treated phosphorylated viscose fabrics, i.e. VP-MPT, exhibited significantly better durability for up to 20 wash cycles compared to VC-MPT fabrics possibly due to better complexation of in situ synthesized metal pyridines with the phosphorylated cellulose. The functionalized fabrics may find applications for topical skin diseases in reducing the necessity of repeated use of antibiotics ointments.

सार

नई कार्यक्षमता सृजित कर टेक्सटाइल में प्रगति की मांग है। हानिकारक यूवी किरणों, प्रदूषण (पार्टिकुलेट मैटर्स), रसायन (अमोनिया, हाइड्रोजन सल्फाइड आदि), सूक्ष्मजीव और अन्य आम तौर पर सामना किए जाने वाले सामयिक मुद्दों जैसे पर्यावरणीय क्षति से पहनने वाले की त्वचा की सुरक्षा के लिए कपड़ा सबसे आकर्षक उम्मीदवार हैं। विश्व स्तर पर, जनसंख्या विभिन्न रोगजनकों के कारण उत्पन्न गंभीर स्वास्थ्य खतरों से पीड़ित है। जैविक हमलों के अलावा, जलवायु परिवर्तन, जैसे ओजोन परत का क्षरण, सूर्य की हानिकारक किरणों (यूवी-ए और यूवी-बी) को पृथ्वी की सतह तक पहुंचने की अनुमति देता है, जिससे त्वचा रोग होते हैं। इसलिए, लोगों की सुरक्षा के लिए प्रभावी बहुक्रियाशील सुरक्षात्मक वस्त्रों का उदय महत्वपूर्ण हो गया है। अनिवार्य पहलू यह है कि कार्यक्षमता को धोने के लिए टिकाऊ होना चाहिए और सबस्ट्रेट के आराम गुणों और सौंदर्यशास्त्र को प्रभावित नहीं करना चाहिए। इस अध्ययन में, सेल्यूलोज के फॉस्फेट व्युत्पन्न को संलग्न कार्यात्मक समूहों को जोड़ने वाले भाग के रूप में खोजा गया है। प्रारंभ में, वायुमंडलीय दबाव प्लाज्मा के तहत सेल्यूलोज के फॉस्फोराइलेशन के लिए एक हरित रसायन दृष्टिकोण की जांच की गई और पारंपरिक थर्मल विधि के साथ तुलना की गई। फॉस्फेट समूहों के लगाव का मूल्यांकन ^{31}P और ^{13}C सॉलिड स्टेट NMR स्पेक्ट्रोस्कोपी और XPS द्वारा किया गया था। थर्मल विधि ने पॉलीमराइज़्ड फॉस्फेट के एक साइड उत्पाद के साथ सेल्यूलोज के मोनोफॉस्फेट का निर्माण किया, जबकि प्लाज्मा विधि ने बिना किसी साइड उत्पाद के केवल मोनोफॉस्फेट का उत्पादन किया। थर्मल उपचार के विपरीत, प्लाज्मा उपचार के बाद विस्कोस कपड़े की उपस्थिति और यांत्रिक गुण लगभग समान रहे। इसके अलावा, प्लाज्मा संशोधित कपड़े की रंगाई अपरिवर्तित रही, जबकि ऊष्मीय रूप से संशोधित कपड़े में यह काफी कम हो गई। फॉस्फोमोलिब्डेट परख द्वारा निर्धारित फॉस्फेट की मात्रा

क्रमशः प्लाज्मा और थर्मल विधियों में 2.88 ± 0.06 और $4.09 \pm 0.19\%$ पाई गई। इस विधि में सेल्युलोज के फास्फारिलीकरण के मौजूदा तरीकों को बदलने की क्षमता है।

इसके अलावा, मजबूत और प्रभावी व्यक्तिगत सुरक्षात्मक कपड़ों की सार्वजनिक स्वास्थ्य मांगों पर विचार करते हुए, एक ज्ञात बैक्टीरियोस्टैटिक और कवकनाशी दवा जिंक पाइरिथियोन (जेडपीटी) का उपयोग करने वाले रोगाणुरोधी कपड़ों की जांच की गई है। ZPT को सेल्युलोसिक फैब्रिक, विस्कोस (VC) पर इन-सीटू संश्लेषित किया गया था, जिसमें जिंक मेटल अग्रदूत और 2-मर्कैटोपाइरीडीन-एन-ऑक्साइड को लिगैंड (VC-ZPT) के रूप में इस्तेमाल किया गया था। तुलना के लिए, ZPT (VP-ZPT) के साथ इन-सीटू क्रियाशीलता से पहले विस्कोस को फॉस्फोराइलेट (VP) भी किया गया था। दोनों दृष्टिकोणों ने रोगाणुओं से पर्याप्त सुरक्षा प्रदान की, हालांकि, फॉस्फेट (वीपी) के साथ सेल्युलोज के कार्यात्मककरण के परिणामस्वरूप सेल्युलोज और जेडपीटी के बीच एक लिंकिंग समूह का निर्माण हुआ, जिसने कपड़े की सतह पर जेडपीटी की बेहतर एकरूपता और धुलाई के लिए उच्च स्थायित्व का प्रदर्शन किया। ICP-MS, SEM और रमन स्पेक्ट्रोस्कोपी द्वारा क्रियाशीलता की पुष्टि की गई थी। इसके अलावा ZPT के साथ फॉस्फेट के बंधन की पुष्टि ^{31}P सॉलिड-स्टेट NMR द्वारा की गई थी। उपचारित कपड़ों के भौतिक गुण, जैसे उपस्थिति, झुकने की लंबाई और यांत्रिक शक्ति अपरिवर्तित रहे। वीपी-जेडपीटी के साथ वीपी-जेडपीटी की रोगाणुरोधी गतिविधियों का अध्ययन ई. कोलाई, एस. ऑरियस और सी. एल्बिकैंस के खिलाफ किया गया था, जो वीपी-जेडपीटी में 20 लॉन्ड्री चक्रों तक प्रभावी पाए गए थे। इसके अतिरिक्त, वीपी-जेडपीटी नमूनों ने कपड़े की सतह पर बैक्टीरिया के खराब पालन का प्रदर्शन किया।

यूवी सुरक्षात्मक गुणों के लिए रोगाणुरोधी धातु पाइरिथियोन परिसरों का पुनः उपयोग सुरक्षात्मक वस्त्रों की प्रयोज्यता को बढ़ाता है। इसलिए, विभिन्न धातु पाइरिथियोन परिसरों के साथ संशोधित सेल्युलोसिक (विस्कोस) वस्त्रों के यूवी-सुरक्षात्मक और रोगाणुरोधी गुणों की भी जांच की गई है। विभिन्न धातु (चांदी

(एजी), सेरियम (सीई), तांबा (सीयू), मैग्नीशियम (एमजी) और जस्ता (जेएन) पाइरिथियोन परिसरों को विस्कोस (वीसी-एमपीटी) के साथ-साथ फॉस्फोराइलेटेड विस्कोस पर संश्लेषित किया गया है। वीपी-एमपीटी)। सतह आकारिकी की विशेषता FE-SEM थी और रासायनिक प्रकृति का अध्ययन XRD, रमन स्पेक्ट्रोस्कोपी, ICP-MS और सॉलिड-स्टेट NMR द्वारा किया गया था। विभिन्न वीसी-एमपीटी और वीपी-एमपीटी उपचारित कपड़ों की रोगाणुरोधी गतिविधियों की तुलना ई. कोलाई, एस. ऑरियस और कैंडिडा एल्बीकैंस से की गई और धातु के आधार पर विभिन्न डिग्री (98-99% तक माइक्रोबियल विकास अवरोध) के लिए प्रभावी पाया गया। उपयोग किया गया। इसके अतिरिक्त, कार्यात्मक कपड़ों में उच्च यूवी अवरोधक गुण पाए गए। उपचारित फॉस्फोराइलेटेड विस्कोस फैब्रिक, यानी वीपी-एमपीटी, वीसी-एमपीटी फैब्रिक की तुलना में 20 वॉश साइकल के लिए काफी बेहतर स्थायित्व प्रदर्शित करता है, संभवतः फॉस्फोराइलेटेड सेल्युलोज के साथ सीटू संश्लेषित धातु पाइरिथियोन के बेहतर संयोजन के कारण। कार्यात्मक कपड़े एंटीबायोटिक मलहम के बार-बार उपयोग की आवश्यकता को कम करने में सामयिक त्वचा रोगों के लिए आवेदन पा सकते हैं।

TABLE OF CONTENTS

CONTENTS	Page No.
Certificate	i
Acknowledgements	iii
Abstract	vii
Table of contents	xv
List of Figures	xxiii
List of Tables	xxxiii
List of Schemes	xxxv
List of Symbols and Abbreviations	xxxvii

Chapter 1 Introduction and literature review

1.1	Introduction	1
1.2	Cellulose	1
1.3	Cellulose properties	2
1.4	Structure of cellulose	3
1.5	Cellulose modifications	3
1.5.1	Carboxymethylation	4
1.5.2	Cellulose sulphate/sulphoethylation	5
1.5.3	Cellulose cationization	6
1.5.4	TEMPO oxidation of cellulose	6
1.5.5	Periodate oxidation of cellulose	7
1.5.6	Cellulose phosphate	8

1.6	Approaches for development of antimicrobial textiles	9
1.7	Techniques used for the development of durable antibacterial textiles	12
1.7.1	Grafting & raft polymerization	14
1.7.2	Triazine trichloride as linker	15
1.7.3	Click chemistry	15
1.7.4	Phosphorylation	16
1.8	Commercial pyrrithione complexes as antimicrobial agents	18
1.9	UV protective textile	19
1.10	Motivation	20
1.11	Objective of the research	21
1.12	Thesis organisation	21

Chapter 2 Phosphorylation of cellulosic textiles by thermal and plasma methods

2.1	Introduction	23
2.2	Experimental section	24
2.1.1	Materials	24
2.1.2	Methods	24
	(a) Thermal method for phosphorylation of viscose	24
	(b) Plasma method for phosphorylation of viscose	25
2.3	Wash durability of phosphorylated viscose fabric	26
2.4	Characterization	26
2.4.1	Physical appearance	26
2.4.2	Field Emission Scanning Electron Microscopy (FE-SEM)	26

2.4.3	ATR-FTIR	26
2.4.4	Nuclear Magnetic Resonance (NMR) Spectroscopy	26
2.4.5	XPS	27
2.4.6	UV-visible spectroscopy	27
2.4.7	XRD	27
2.4.8	Thermogravimetric Analysis (TGA)	27
2.4.9	Tensile testing	28
2.4.10	Softness	28
2.4.11	Drop absorbency and dye-ability	28
2.5	Results and Discussion	28
2.5.1	Phosphorylation of cellulose by thermal and plasma methods	28
2.5.2	Surface morphology	33
2.5.3	Chemical Characterization	35
2.5.4	Physical Characterization	54

Chapter 3. In situ synthesis of zinc pyrithione on cellulosic textiles for antimicrobial applications

3.1	Introduction	61
3.2	Experimental Section	61
3.2.1	Materials	61
3.2.2	Methods	62
	a) In-situ synthesis of VC-ZPT	62
	b) In-situ synthesis of VP-ZPT	62

3.3	Wash durability	63
	3.4 Antimicrobial activity	63
	3.4.1 Qualitative antibacterial Kirby-Bauer disk diffusion method	63
	3.4.2 Quantitative antibacterial method	64
	a) Growth inhibition of bacteria (% Reduction)	64
	b) Bacteria survival	65
	c) Fabric damage and adherence of bacteria	65
	3.4.3 Quantitative antifungal assay	66
3.5	Characterization	66
	3.5.1 Physical properties	66
	(a) Appearance	66
	(b) Feel	68
	(c) Breaking strength	68
	3.5.2 Morphology and Chemical Properties	68
	(a) Morphology	68
	(b) Chemical structure	68
	(c) Stability	69
3.6	Quantification of ZPT	69
3.7	Results and Discussion	69
	3.7.1 In-situ synthesis of ZPT on control and phosphorylated viscose fabric	69
	3.7.2 Chemical characterisation	73

	(i) Determination of crystallographic structure of ZPT synthesised on fabric	73
	(ii) Chemical interaction of ZPT with viscose fibre	74
	(iii) Mapping of ZPT on the surface of textiles	77
	(iv) Bonding of ZPT with phosphate linker	80
3.7.3	Physical characteristics	83
	(i) Surface morphology	83
	(ii) Feel	85
	(iii) Mechanical properties	86
3.8	Wash Durability	87
3.9	Stability	88
	3.9.1 Thermal Stability	88
	3.9.2 Photo stability	90
3.10	Antimicrobial activity	90
	3.10.1 Qualitative evaluation	90
	3.10.2 Quantitative evaluation	95
	3.10.3 Bacterial adherence and fabric damage	100

Chapter 4 In situ synthesis of pyrrithione complexes with different metal ions (Ag, Ce, Mg, Cu) on cellulosic textiles

4.1	Introduction	105
4.2	Experimental Section	105
	4.2.1 Materials	105

4.2.2	Method	106
	a.) In-situ synthesis of metal (Ag, Ce, Mg, Cu and Zn) pyrrithione complex on viscose (VC-MPT) fabric	106
	b.) In-situ synthesis of metal (Ag, Ce, Mg, Cu and Zn) pyrrithione complex on phosphorylated viscose (VP-MPT) fabric	106
4.3	Characterization	107
4.4	Wash durability	107
4.5	Results and Discussion	109
	4.5.1 In situ synthesis of metal (Ag, Ce, Mg, Cu and Zn) pyrrithione complexes on VC and VP	109
	4.5.2 Wash durability by quantification of MPT on fabric	109
	4.5.3 Appearance of fabric	112
	4.5.4 Surface morphology	112
	4.5.5 Interaction and bonding of metal pyrrithione complexes with VC and VP	119
	4.5.6 Crystal structure of VC-MPT and VP-MPT fabric	129

Chapter 5 Comparison of different pyrrithione complexes for antimicrobial and UV protective textiles

5.1	Introduction	133
5.2	Experimental Section	133
	5.2.2 Methods	133
	5.2.3 Characterisation	134

i) UV radiation blocking of fabric and its mechanism	134
ii) Qualitative and quantitative antimicrobial activity	134
5.3 RESULTS AND DISCUSSION	134
5.3.1 UV- blocking property of VC-ZPT and VP-ZPT fabric	134
5.3.2 Antimicrobial activity	141
a) E. coli	146
b) S. aureus	147
5.3.3 Fabric damage	149
5.3.4 Antifungal activity	149
5.3.5 Mechanism of antimicrobial activity	158
Chapter 6 Conclusions	159
References	163
Author resume	181

LIST OF FIGURES

Figure No.	Caption of the Figure	Page No.
Figure 1.1	Morphology of cotton fabric and its chemical structure of cellulose.	3
Figure 1.2	Cellulose modification to its various derivatives	4
Figure 1.3	Traditional antibacterial agents	10
Figure 1.4	Commercial pyrithione complexes a) Zinc pyrithione and b) copper pyrithione	18
Figure 2.1	Photographs of thermal phosphorylation of viscose fabrics treated with DAHP at cellulose to DAHP ratio of a) 1:0 b) 1:0.5, c) 1:1, and d) 1:2.0. Plasma phosphorylated viscose fabrics treated with DAHP at cellulose to DAHP ratio of e) 1:0, f) 1:0.5, g) 1:1, and h) 1:2.0	29
Figure 2.2	Plot of reflectance as a function of reagent concentration used for phosphorylation of viscose fabric using the two methods	30
Figure 2.3	Plot of whiteness index as a function of reagent concentration used for phosphorylation of viscose fabric using the two methods	31
Figure 2.4	SEM images of thermally treated viscose at different molar ratios of cellulose : DAHP a) Control, b) 1:0.5, c) 1:1 and d) 1:2.0	34

Figure 2.5	SEM images of plasma treated viscose at different molar ratios of cellulose: DAHP a) Control, b) 1:0.5, c) 1:1 and d) 1:2.0	35
Figure 2.6	ATR-FTIR spectra of control and phosphorylated fabric by a) Thermal method and b) Plasma method	36
Figure 2.7	Solid-state single pulse decoupled ^{31}P NMR spectra of phosphorylated viscose as prepared by a) thermal and b) plasma methods at different concentrations	38
Figure 2.8	Solid-state single pulse decoupled ^{31}P NMR spectra of washed phosphorylated viscose fabrics a) Thermal method, and b) Plasma method	39
Figure 2.9	Solid state single-pulse decoupled ^{13}C NMR spectra of phosphorylated viscose fabrics a) Thermal method, and b) Plasma method	41
Figure 2.10	XPS overall spectra of untreated control viscose and phosphorylated viscose by thermal method and by plasma method (Cellulose: DAHP = 1:1)	42
Figure 2.11a	High resolution C 1s spectra of untreated control viscose	43
Figure 2.11b	High resolution C 1s spectra of phosphorylated viscose by (i) thermal method and (ii) plasma method (Cellulose: DAHP = 1:1)	44
Figure 2.12a	High resolution O1s spectra of untreated a) control viscose	46

Figure 2.12b	High resolution O1s spectra of phosphorylated viscose by i) thermal method and by ii) plasma method (Cellulose: DAHP = 1:1)	47
Figure 2.13	High resolution P2p spectra of phosphorylated viscose by a) thermal method and b) plasma method (Cellulose: DAHP = 1:1)	49
Figure 2.14	Calibration plot measured at 823 nm using standard phosphate salt	50
Figure 2.15	UV vis phosphomolybdate assay spectra multiple samples of a) VP(2.0)-T (Thermal method) and b) VP(2.0)-P (Plasma method)	51
Figure 2.16	UV-vis plots of the methanol washed samples	52
Figure 2.17	³¹ P solid-state NMR spectrum of VP(2.0)-P after 180 days of ageing	53
Figure 2.18	XRD spectra of control and VP(2.0) of phosphorylated samples by thermal and plasma method.	54
Figure 2.19	Thermogravimetric plots for samples prepared using different reagent concentration a) thermal method, b) plasma method	56
Figure 3.1	Photographic images of control and treated fabrics	72
Figure 3.2	Reflectance of the curve of the control viscose and ZPT treated fabric on neat (VC-ZPT) and phosphorylated viscose (VP-ZPT)	72
Figure 3.3	XRD spectra of various samples	73

Figure 3.4	Raman spectra of various samples	74
Figure 3.5	Deconvoluted Raman peaks in the region 950-1550 cm^{-1} for various samples	76
Figure 3.6	Raman mapping image of ZPT at 830, 1548 and 1605 cm^{-1} synthesized on (a) VC and (b) VP. (Magnification of the inset box is $\sim 50 \mu\text{m}$)	78
Figure 3.7	EDX mapping of elements present in (a) control viscose (VC) with carbon and oxygen, (b) phosphorylated viscose (VP) with phosphorus, (c) ZPT synthesized on cellulosic viscose (VC-ZPT) with zinc and sulphur, and (d) ZPT synthesized on phosphorylated viscose (VP-ZPT) with zinc, sulphur, carbon and phosphorus	79
Figure 3.8	Solid-state ^{31}P -NMR of zinc phosphate powder compound, VP and VP-ZPT fabric	81
Figure 3.9	Solid-state ^{13}C -NMR of ZPT powder	82
Figure 3.10	Solid state ^{13}C -NMR of VC, VC-ZPT and VP-ZPT fabric	83
Figure 3.11	SEM images showing surface morphologies of (a) control viscose, (b) phosphorylated viscose (c) VC-ZPT, and (d) VP-ZPT fabric	84
Figure 3.12	Bending length of control viscose, VC-ZPT and VP-ZPT along warp and weft direction of fabric	86
Figure 3.13	Breaking strength of control viscose, VC-ZPT and VP-ZPT along warp and weft direction of fabric	87

Figure 3.14	Weight % of ZPT complex on the weight of functionalized fabrics as a function of washing cycles	88
Figure 3.15	Thermogravimetric analysis of the samples	89
Figure 3.16	Photo stability of ZPT extracted from (a) VC-ZPT and (b) VP-ZPT	91
Figure 3.17	Qualitative antibacterial zone inhibition of samples with increase in laundry cycles against E. Coli	92
Figure 3.18	Qualitative antibacterial zone inhibition of samples with increase in laundry cycles against S. aureus	93
Figure 3.19	Qualitative antibacterial zone inhibition of (i) control viscose (VC), (ii) phosphorylated viscose (VP) and (iii) ZPT synthesized on cellulosic viscose (VC-ZPT) and (iv) phosphorylated viscose (VP-ZPT) against Candida albicans	94
Figure 3.20a	Quantitative optical density (absorbance) of growth solution of samples with increase in laundry cycles against E. coli (GC represents the growth control without fabric)	95
Figure 3.20b	Quantitative optical density (absorbance) of growth solution of samples with increase in laundry cycles against S. aureus (GC represents the growth control without fabric)	96
Figure 3.21	Quantitative optical density (absorbance) of growth solution of samples with increase in laundry cycles against Candida. albicans	97

Figure 3.22	Number of survived CFU from the growth solution of control and ZPT synthesized on cellulosic viscose (VC-ZPT) and phosphorylated viscose (VP-ZPT) with increase in washing cycles (0,10 and 20) against E. coli	98
Figure 3.23	Number of survived CFU from the growth solution of control and ZPT synthesized on cellulosic viscose (VC-ZPT) and phosphorylated viscose (VP-ZPT) with increase in washing cycles (0,10 and 20) against S. aureus	99
Figure 3.24	Photographs showing the growth of bacteria on the control (VC), VC-ZPT-20W and VP-ZPT-20W fabric against a) E. coli b) S. aureus	101
Figure 3.25	Electron images (right column) showing the adherence of bacteria on the surface of fabrics against a) E. coli b) S. aureus	102
Figure 4.1	Add-on percentage of metal pyrithione complexes on (i) VC and (ii) VP substrates	110
Figure 4.2	Photographic images of the fabrics synthesized with different metal (Ag, Ce, Mg, Cu and Zn) pyrithione complexes on a) cellulosic viscose (VC), b) phosphorylated viscose (VP)	111
Figure 4.3	Reflectance curves of the fabrics synthesized with different metal (Ag, Ce, Mg, Cu and Zn) pyrithione complexes on a) cellulosic viscose (VC), b) phosphorylated viscose (VP)	113

Figure 4.4	Electron micrographs of VC-MPT (i) control viscose (VC), (ii) VC-CuPT (iii) VC-ZPT (iv) VC-AgPT (v) VC-CePT (vi) VC-MgPT showing surface morphologies of the samples	115
Figure 4.5	Electron micrographs of VP-MPT (i) phosphorylated viscose (VP), (ii) VP-CuPT (iii) VP-ZPT (iv) VP-AgPT (v) VP-CePT (vi) VP-MgPT showing surface morphologies of the samples	116
Figure 4.6	EDX elemental mapping of VC-MPT	117
Figure 4.7	EDX elemental mapping of VP-MPT sample	118
Figure 4.8	Raman spectra of MPT-fabric samples synthesized using metals (Ag, Ce, Mg, Cu and Zn), (a) VC-MPT, b) VP-MPT	120
Figure 4.9	Raman deconvoluted spectra of control viscose fabric	121
Figure 4.10	Raman deconvoluted spectra of the AgPT metal pyrrithione complexes synthesized on (i) cellulosic viscose (VC) and (ii) phosphorylated viscose (VP)	122
Figure 4.11	Raman deconvoluted spectra of the CePT metal pyrrithione complexes synthesized on (i) cellulosic viscose (VC) and (ii) phosphorylated viscose (VP)	123
Figure 4.12	Raman deconvoluted spectra of the MgPT metal pyrrithione complexes synthesized on (i) cellulosic viscose (VC) and (ii) phosphorylated viscose (VP)	124
Figure 4.13	Raman deconvoluted spectra of the CuPT metal pyrrithione complexes synthesized on (i) cellulosic viscose (VC) and (ii) phosphorylated viscose (VP)	125

Figure 4.14	Raman deconvoluted spectra of the ZPT metal pyrithione complexes synthesized on (i) cellulosic viscose (VC) and (ii) phosphorylated viscose (VP)	126
Figure 4.15	Single-pulsed decoupled ^{31}P solid-state NMR spectra of VP-MPT	129
Figure 4.16	XRD spectra of (a) VC-MPT (b) VP-MPT fabrics synthesized with different metal ions Ag, Ce, Mg, Cu and Zn in comparison with control viscose	130
Figure 5.1	Comparison of UV transmission of control viscose (VC) and 0 wash fabrics AgPT, CePT, MgPT, CuPT and ZPT synthesized on a) VC and b) VP	135
Figure 5.2	Comparison of UV transmission of control viscose (VC) and 10 wash fabrics AgPT, CePT, MgPT, CuPT and ZPT synthesized on a) VC and b) VP	138
Figure 5.3	Comparison of UV transmission of control viscose (VC) and 20 wash fabrics AgPT, CePT, MgPT, CuPT and ZPT synthesized on a) VC and b) VP	139
Figure 5.4a	UPF rating as a function of washing cycles of VC-MPT in comparison to VC	140
Figure 5.4b	UPF rating as a function of washing cycles of VP-MPT in comparison to VC	141

Figure 5.5	Qualitative zone of inhibition of (i) VC-MPT-0W, (ii) VP-MPT -0W, (iii) VC-MPT-10W and (iv) VP-MPT-10W fabric against a.) E. coli and b.) S. aureus	142
Figure 5.6	Absorbance values of growth media for quantitative assessment of antibacterial activity of Pyrithione complex synthesis on VC and VP (i) AgPT, (ii) CePT, (iii) MgPT, (iv) CuPT and (v) ZPT against E. coli	143
Figure 5.7	Absorbance values of growth media for quantitative assessment of antibacterial activity of Pyrithione complex synthesis on VC and VP (i) AgPT, (ii) CePT, (iii) MgPT, (iv) CuPT and (v) ZPT against S. aureus	144
Figure 5.8a	Percentage inhibition of E. coli bacterial growth on VC-MPT fabrics	145
Figure 5.8b	Percentage inhibition of E. coli bacterial growth on VP-MPT fabrics	146
Figure 5.9	Percentage inhibition of S. aureus bacterial growth on a) VC-MPT & b) VP-MPT fabrics	148
Figure 5.10a	Fabric damage due to E.coli bacteria growth on control viscose and 20 wash VC-MPT complex treated fabrics	150
Figure 5.10b	Fabric damage due to E.coli bacteria growth on control viscose and 20 wash VP-MPT complex treated fabrics	151
Figure 5.11a	Fabric damage due to S. aureus bacteria growth on control viscose and 20 wash VC-MPT complex treated fabrics	152

Figure 5.11b	Fabric damage due to <i>S. aureus</i> bacteria growth on control viscose and 20 wash VP-MPT complex treated fabrics	153
Figure 5.12	Visualization of bacteria colonization under SEM of control viscose and 20 wash CuPT synthesized fabric on VC and VP	154
Figure 5.13a	Absorbance values of growth media for quantitative assessment of antifungal activity against <i>Candida albicans</i> of Metal (Ag, Ce, Mg, Cu, Zn) Pyrithione complexes synthesized on VC	155
Figure 5.13b	Absorbance values of growth media for quantitative assessment of antifungal activity against <i>Candida albicans</i> of Metal (Ag, Ce, Mg, Cu, Zn) Pyrithione complexes synthesized on VP	156
Figure 5.14	Percentage inhibition of fungal growth <i>Candida albicans</i> on a) VC-MPT and b) fabrics	157

LIST OF TABLES

Table No.	Title of the Table	Page No.
Table 1.1	Reported methods for phosphorylation of cellulose	16
Table 2.1	Analysis of appearance of fabric samples using dE	33
Table 2.2	Relative peak intensities of C1s (C-C*, C*-O and O-C*-O) bonds of various samples prepared at Cellulose: DAHP 1:1 after washing	45
Table 2.3	Mechanical properties of the control and treated samples	57
Table 2.4	Bending lengths for control and treated samples	58
Table 3.1	Assignment of peaks observed in Raman Spectra	75
Table 4.1	Shifts in Raman peaks of VC-MPT and VP-MPT as compared to control fabric.	127
Table 5.1	Percent transmission of UV-A and UV-B region of VC-MPT and VP-MPT fabric	136

List of Schemes

Scheme No.	Title of the Scheme	Page No.
Scheme 1.1	Carboxymethylation of cellulose	5
Scheme 1.2	Sulphation of cellulose	5
Scheme 1.3	Cationization of cellulose	6
Scheme 1.4	Carboxylation of cellulose by TEMPO oxidation	7
Scheme 1.5	Aldehyde derivative of cellulose by periodate oxidation	8
Scheme 1.6	Phosphorylation of cellulose	8
Scheme 2.1	Schematic representation of phosphorylation of viscose fabric by thermal and plasma method	29
Scheme 2.2	Possible mechanism of phosphorylation of cellulose.	32
Scheme 3.1	Schematic of quantitative Antibacterial test methods	67
Scheme 3.2	Schematic representation of In-situ synthesis of ZPT on control viscose and phosphorylated viscose fabrics	71
Scheme 3.3	Reaction scheme for the synthesis of ZPT on VP	71
Scheme 4.1	Schematic representation of in situ synthesis of metal (Ag, Ce, Cu, Mg, Zn) pyrithione complex on cellulosic and phosphorylated viscose fabrics	108

LIST OF SYMBOL AND ABBREVIATIONS

Symbol/Abbreviation	Expanded Form/Term
VC	Control viscose
VP	Phosphorylated viscose
PT	Pyrithione
ZPT	Zinc pyrithione
VC-ZPT	Zinc pyrithione synthesised on control viscose
VP-ZPT	Zinc pyrithione synthesised on phosphorylated viscose
CuPT	Copper pyrithione
CePT	Cerium pyrithione
MgPT	Magnesium pyrithione
AgPT	Silver pyrithione
DAHP	Diammonium hydrogen phosphate
NMR	Nuclear magnetic resonance
MAS	Magic angle spinning
CP/MAS	Cross polarization magic angle spinning
XPS	X-ray photoelectron spectroscopy
UV	Ultraviolet
^{31}P	Phosphorus-31 nuclei
^{13}C	Carbon-13 nuclei
cm^{-1}	Wavenumber unit
MHz	Megahertz

ppm	Parts per million
eV	Electron volt
∂	Del
Å	Angstrom
μm	Micro meter
$^{\circ}\text{C}$	Degree Celsius
α	Alpha
β	Beta